Gravitational lensing: a unique tool for cosmology
ASP Conference Series, Vol. xxx, 2003
D. Valls–Gabaud and J.–P. Kneib (eds.)

Quasar Lensing: the Observer's Point of View

F. Courbin
Institut d'Astrophysique et de Géophysique, Université de Liège, Allée du 6 août 17, Bat B5C, Liège 1, Belgium

Abstract. The determination of the Hubble parameter H_0 is probably one of the most important applications of quasar lensing. The method, based on the measurement of the so-called "time-delay" between the lensed images of distant sources, e.g., quasars, and on detailed mass modeling of the potential well responsible for the multiple images, yields an accuracy at least comparable with other techniques and that can be improved further with high precision observations, as can be obtained with intrumentation of constantly increasing quality. The basics of the "time-delay" method are described, and the emphasis is put on the observational constraints available to the astrophysicist in order to implement the method and to derive an accurate value for H_0, independent of any standard candle or any strong prior on the other cosmological parameters.

1. Why Observing Lensed Quasars ?

Gravitational lensing is a well established field of astrophysics. It is well enough understood that it can be applied to other areas of astrophysics in order to tackle astrophysical problems under a new angle. Some applications of gravitational lensing concentrate on the study of the objects responsible for the deflection of light, the *lenses*. Others, aim at studying the stretched, distorted and (de)magnified images of the background objects, the *sources*. For example, stellar micro-lensing is used to probe the content of our own galaxy in dark low-mass stars, or micro-lenses. The weak distortions of very distant galaxies is used to detect indirectly and even to map what might be the largest lenses in the Universe: the Large Scale Structures. In many multiply imaged quasars, (micro)lenses are found within (macro)lenses: quasar micro- or milli-lensing provides us with information on the structure of both the sources and the lenses (see for example Schechter 2003; Wambsganss 2003).

Many of the applications of gravitational lensing, and in particular of quasar lensing, were known and described decades ago. They nevertheless only start now to be implemented on a systematic basis, taking advantage of the recent explosion of the number of large observatories that operate at high angular resolution and down to very faint magnitudes.

Quasar lensing helps us to study lenses and sources, but it also consists in a fantastic tool to study the space between the lenses and the sources ! While the light travels from the source to the observer, it is absorbed by the Inter Stellar Medium of the lens, and by the neutral gas of the Inter-Galactic Medium. The

study of absorption lines in multiply imaged quasars provides us with information about the geometry of intergalactic clouds (Smette 2003). Last, but not least, multiply imaged quasars tell us about the size of the Universe, through the measurement of the so-called "time-delay" between the lensed images. This quantity is directly related to the mass distribution in the lensing galaxy and to the Hubble parameter H_0. The measurement of H_0 using lensed quasars is the topic of the present chapter.

2. First Discoveries and Searches

2.1. A Few Lucky Cases

The observational history of lensed quasars starts with a few lucky cases found "by accident" during surveys or follow-up observations of projects unrelated to gravitational lensing. The very first case was the double quasar Q 0957+561. When observed at optical wavelengths, the z=1.405 quasar appeared as two point sources separated by 5.7″ (Walsh et al. 1979). Spectra obtained with the Multi-Mirror-Telescope showed that both objects had almost identical spectral properties (Weymann et al. 1979), strongly supporting the hypothesis of gravitational lensing: two images of one single object were seen, due to the potential well created by a galaxy along the line of sight. In fact, not only the spectra were identical, but subtraction of the quasar images also revealed, for the first time, the lensing galaxy, hidden by the much brighter quasar images. With such observational material, no serious doubts could remain about the lensed nature of Q 0957+561.

Other cases were found soon after, such as the quadruply imaged quasar PG 1115+080 (Weymann et al. 1980) that we will use in this article to illustrate how lensed quasars can help use to determine H_0. Even the famous "Einstein Cross", Q 2237+0305 (Huchra et al. 1985; see Fig. 1), was discovered during follow-up observations in the course of the CfA redshift survey: a spectrum obtained of the central parts of a z=0.04 redshift galaxy, turned out to display the exact characteristics of a quasar at much higher redshift, z=1.7. In addition, the total apparent luminosity of the bulge of the galaxy was far too high for a normal spiral. Indeed, it was in fact the combined light of the actual galaxy's bulge and of the four (unresolved) quasar images. High resolution images taken a few years later nicely confirmed that the object was composed of four separate quasar images almost aligned with the bulge of the spiral galaxy (Schneider et al. 1988; see Fig. 2).

2.2. Systematic Searches and the Magnification Bias

While the very first lenses were found by chance (and there are still lenses found by chance from time to time; see for example Sluse et al. 2003), observational strategies were soon designed to find many more, on purpose !

Such an enterprise requires to estimate the number of lensed objects within a sample of quasars, given the selection criteria, in general a flux limit. The exercise has been done many times by many groups, following the ideas first proposed by Turner (1980). The original idea of Turner was to describe the effect of undetected lenses on the apparent evolution of quasars. As lensing amplifies

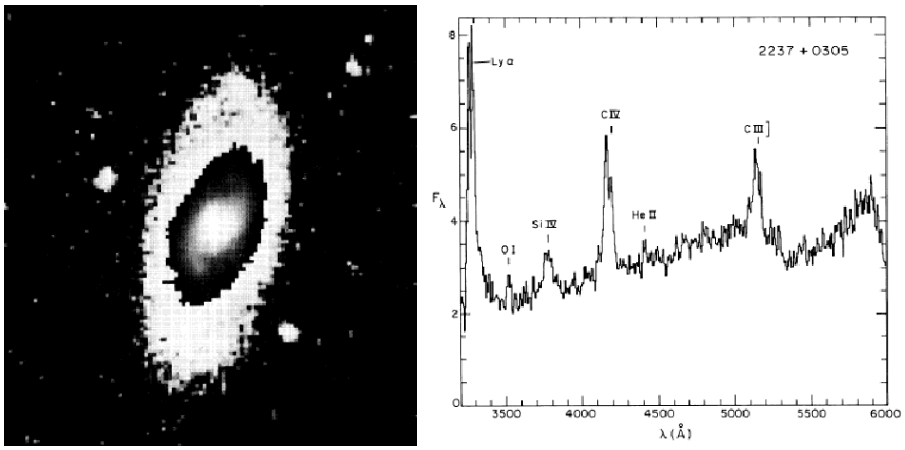

Figure 1. *Left:* ground based image of the lensing galaxy (z=0.04) in the Einstein Cross. The spatial resolution is low. It does not allow to discriminate between the bulge of the galaxy and any background quasar image(s). *Right:* spectrum of the most central part of the galaxy. The spectrum is not the one of a low redshift galaxy, but that of a much more distant object: a quasar at z=1.7 (Huchra et al. 1987).

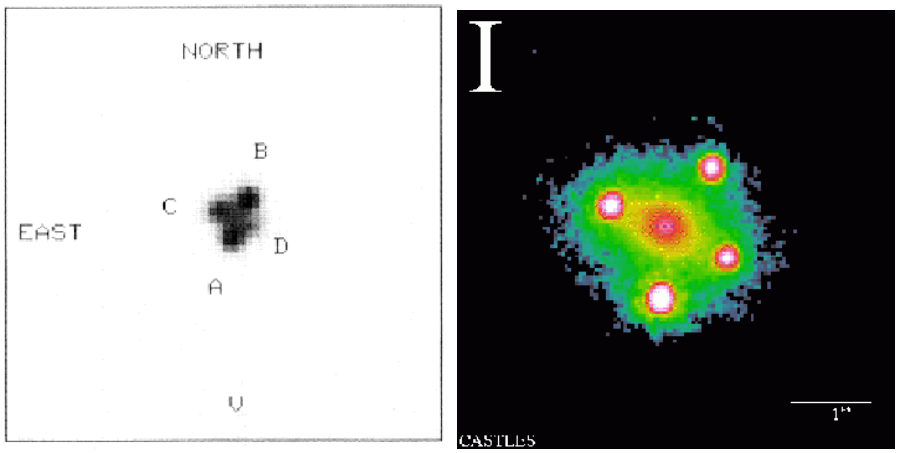

Figure 2. *Left:* ground based image of the "Einstein cross" unveiling, for the first time, four separated quasar images. The field of view 10″wide (Schneider et al. 1988). *Right:* HST view of the Einstein cross, allowing for accurate astrometry and photometry of the system as well as detailed surface photometry of the bulge of the lensing galaxy. The length of the white bar at the bottom right is 1″ (Image taken from Kochanek et al. 2003a).

the apparent luminosity of background objects, significant modifications of the observed luminosity function of quasars were suspected, in particular toward the bright end. Several ingredients are needed to carry out the calculation: (1) the spatial distribution of lenses, (2) the spatial distribution of sources, (3) a realistic mass model for the lenses in order to estimate the amplification, (4) a cosmological model and, (5) the (unlensed) luminosity function of the sources. Although none of these were precisely known in the eighties, it was quickly understood that lens statistics was a particularly sensitive function of the slope of the source luminosity function: the relative weights of the faint to bright quasar number counts give rise to the so-called "magnification bias" (see contribution by Smette, 2003 for more details). Its net effect on a flux limited sample is that the fraction of sources likely to be magnified by a given amount μ is higher for apparently bright sources than for fainter ones (see for example Schneider, Ehlers & Falco, 1992). In other words, bright sources are seen bright, because they are (more likely to be) lensed.

Based on this simple, but important finding, several surveys were started, targeting at quasars with the brightest absolute magnitude in large samples. Because at the time of the first surveys were initiated, high angular resolution was easier to achieve in the radio than in the visible, multiply imaged quasars were often the found in large radio surveys (e.g., Lawrence et al. 1986; Langston et al. 1989; Hewitt et al. 1992). The largest of these surveys so far are probably CLASS, the "Cosmic Lens All Sky Survey" and JVAS, the "Jorell Bank - VLA Astrometric Surveys" (see, among others, Patnaik et al. 1992; Myers et al. 1995; Jackson et al. 1998).

Almost in parallel with radio surveys, optical searches started and successfully yielded a significant harvest of multiply imaged quasars. Among the first ones to be discovered, were the double UM 673 (Surdej et al. 1987), the quadruple "cloverleaf" H 1413+117 (Magain et al. 1988), followed by some cases in the Hamburg/ESO survey for bright quasars (e.g., Wisotzki et al. 1993). The search for new cases is still ongoing, with a success rate that makes it difficult to keep track of every new discovery. Large multi-wavelengths wide field surveys are now relatively easy to carry out and the "multiband" magnification bias is studied in order to understand the effect of lensing on such data (Wyithe et al. 2003). The prospects to find many new lenses suitable for cosmological applications (e.g., in SLOAN, FIRST, GOODS, etc...) are therefore excellent. At the time of the writing of this article, several new good candidates from these surveys are under analyze.

3. Lensed Quasars and H_0

Quasar lensing helps to solves astrophysical puzzles in various ways, but one of its most beautiful applications is probably the determination of the Hubble parameter H_0.

3.1. The Time-delay Method

In 1964, the Norwegian astronomer Sjur Refsdal proposed an original method (Refsdal 1964) to use gravitational lensing as a tool to measure the size/age of the Universe. When photons propagate from a distant source toward the observer,

they are under the effect of the gravity field of lenses along the line of sight. They do not follow a straight line anymore, but their trajectory is curved and longer than the original one. As a consequence, it takes more time for the photons to travel from a lensed source than from an unlensed one. The *geometrical* difference introduced by the lens between the two, lensed and unlensed paths, introduces a time-lag between the arrival times of the (lensed and unlensed) photons at the position of the observer. This time lag is called the geometrical "time-delay", $t_{\rm geom}$. While passing in the immediate vicinity of the gravity field of the lens, the light is affected by a second delay: the gravitational time-delay, $t_{\rm grav}$. A "lensed photon" will be seen by an observer with a total time-delay $t_{\rm tot} = t_{\rm geom} + t_{\rm grav}$, with respect to the observation of the same photon if it were not lensed.

The time-delay is a function of image position in projection on the plane of the sky. One can then define an *arrival time surface* that associates, to each position on the sky, a given a value of the time-delay. Most of this surface is missed by the observer who has only access to the few areas where the lensed images form. When two or more images of the source are observed it is possible to compare the arrival times at the positions of the lensed images and to determine a "relative time-delay". This is in fact the only truly measurable quantity, rather than the actual time-delay between the lensed and unlensed paths to the source, since the unlensed source is never visible.

In practice, time-delays are measured taking advantage of a lensed source with significant photometric variations. Due to the time-delay, the variations will be detected by the observer at different times in the light curves of each image. The shift in time between the light curves is simply the (total) time-delay between the images. Refsdal (1964) proposed to measure time-delays in lensed supernovae, but his method was published just when the first quasars were discovered (Schmidt 1963). Quasars, that later turned out to be very numerous in the sky, rather bright, and photometrically variable, were promising objects to measure time-delays if at least some of them were found to be lensed. They appeared in any case much more promising than rare and transient phenomena such as supernovae. Indeed, thousands of quasars are now known, and several tens of them are lensed. Measured quasar time-delays span over a broad range of values, between days and months. One is larger than a year: Q 0957+561 (e.g., Vanderriest et al. 1989).

3.2. Constraints and Uncertainties

Time-delays can be predicted from lens modeling, for any observed image configuration and compared with the measured ones in order to infer the value of H_0. The task requires detailed observations, deep, and at high angular resolution, and a good mass model for the lensing galaxy, as can be seen from the explicit expression for the time-delay in equations (1-3). A full description of the calculation can be found in Schneider, Ehlers & Falco (1992). We only use the result here to illustrate how observations help to achieve our goal. As explained above, the total time delay is the sum of two contributions, so that:

$$t_{\rm tot} = t_{\rm geom} + t_{\rm grav}, \tag{1}$$

Each contribution to the total time-delay writes as:

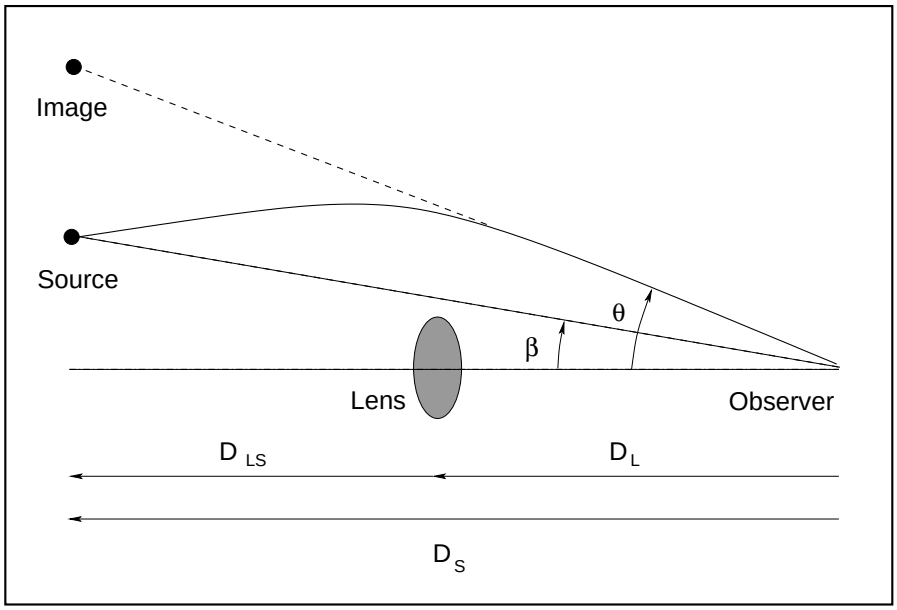

Figure 3. Schematic view of a lensed quasar, with only one image represented. The difference in length between the straight (dashed) and curved (solid) lines is only responsible for the geometrical time-delay. The total time-delay also includes a gravitational part that depends on the mass distribution in the lensing galaxy (see equations 1-3).

$$t_{\rm geom}(\vec{\theta}) = (1+z_{\rm L})\frac{D_{\rm L}D_{\rm S}}{cD_{\rm LS}}(\vec{\theta}-\vec{\beta})^2, \tag{2}$$

$$t_{\rm grav}(\vec{\theta}) = (1+z_{\rm L})\frac{8\pi G}{c^3}\nabla^{-2}\Sigma(\vec{\theta}). \tag{3}$$

where z_L is the redshift of the lensing galaxy. As illustrated in Fig. 3, the angle $\vec{\theta}$ (in 2D in real cases) gives the position of the images on the plane of the sky and β is the angular position of the source.

The Hubble parameter H_0 is contained in the geometrical part of the time-delay, through the angular diameter distances to the lens D_L, to the source D_S and through the distance between the lens and the source, D_{LS}.

Equation (3), the gravitational part of the time-delay, depends only on well known physical constants, and on the inverse of the 2D Laplacian of the mass density profile in the lensing galaxy $\Sigma(\vec{\theta})$. In other words, it strongly depends on the shape of the 2D mass profile of the lens (ellipticity, position angle), and on its slope. We will see later that the main source of uncertainty on the gravitational part of the time-delay comes from the *radial slope* of the mass distribution.

Several of the ingredients necessary to compute the time-delay can be precisely measured from observations. Although every lensed system has its own

particularities, the positions of the lensed images defined by $\vec{\theta}$ are usually the easiest quantities to constrain. With present day instrumentation, an accuracy of a few milli-arcsec is reached. The position of the lensing galaxy relative to the quasar images, when it is not double or multiple can be of the order of 10 milli-arcsec. As for the position $\vec{\beta}$ of the source relative to the lens, it is usually free in lens models. No observation can constrain it.

In most cases, astrometry is not a major limitation to the use of lensed quasars. However, image configurations that are very symmetric about the center of the lens are more sensitive to astrometric errors than assymetric configurations. Let us assume that $\vec{\beta}$ is very small compared with $\vec{\theta}$ (i.e., the source is almost aligned with the lens and the observer). Lets then consider a doubly imaged quasar with two images located at positions $\vec{\theta_1}$ and $\vec{\theta_2}$ away from the lens, and separated by $\vec{\theta}$. The geometrical time-delay between the two images is:

$$\begin{aligned} \Delta t_{\rm geom} = t(\vec{\theta_1}) - t(\vec{\theta_2}) &\simeq (1+z_{\rm L})\frac{D_{\rm L}D_{\rm S}}{cD_{\rm LS}}(\vec{\theta_1^2} - \vec{\theta_2^2}) \\ &= (1+z_{\rm L})\frac{D_{\rm L}D_{\rm S}}{cD_{\rm LS}}\left[\vec{\theta}\cdot(2\vec{\theta_1} - \vec{\theta})\right]. \end{aligned} \quad (4)$$

If we now consider that the error on the image separation $\vec{\theta}$ is much smaller than the error on the position of image 1 relative to the lens, $\vec{\theta_1}$, we can approximate the error on the time-delay. Since the errors $d\vec{\theta_1}$ and $d\vec{\theta}$ on $\vec{\theta_1}$ and $\vec{\theta}$ are not much correlated, they propagate on the time-delay as

$$\frac{d\Delta t_{\rm geom}}{\Delta t_{\rm geom}} \simeq \frac{2}{(|2\vec{\theta_1} - \vec{\theta}|)} d\theta_1. \quad (5)$$

In symmetric configurations, where the lens is almost midway between the images, $2|\vec{\theta_1}| \simeq |\vec{\theta}|$, so that the denominator in equation (5) is zero or close to it, leading to large relative errors on the time-delay, and hence on H_0, whatever mass model is adopted for the lensing galaxy.

The advantage of symmetric configurations over assymetric ones is that they often have more than two lensed images (the source is more likely to be within the area enclosed by the radial caustic; see previous chapters on the basics of quasar lensing), offering the opportunity to measure several time-delays per system. The drawback is a larger sensitivity to astrometric errors.

Redshift information is also of capital importance in the calculation of the time-delay. Time-delays are proportional to $(1+z_{\rm L})$ as seen in equation (4). The angular diameter distances also depend on the redshift of the lens and source $z_{\rm L}$ and $z_{\rm S}$. Both should therefore be measured carefully. Although the lens and source redshifts are available for most know system, their measurement is not as straightforward as one could expect. Given the small separation between the lensed images and the high luminosity contrast between the source and lens, obtaining a spectrum of the lens is often challenging and may involve significant struggling with the data (e.g., Lidman et al. 2000). In other cases, for example in systems discovered in the radio, one faces the opposite situation: the optical

counterpart of the source is so faint that no spectrum can be obtained of it, while the lens is well visible (e.g., Rusin et al. 2001).

Finally, the other cosmological parameters such as Ω_Λ and Ω_0 also play a role in the calculation of the time-delay, through the angular diameter distances. The dependence of the distances on (Ω_Λ,Ω_0) is however very weak. In addition, other methods (Supernovae, CMB) seem much better at pinning down their values than quasar lensing does. One shall therefore use the known values of (Ω_Λ,Ω_0) in quasar lensing and infer H_0, to which it is much more sensitive.

3.3. The Mass Model and Degeneracies

Most unknowns in the calculation of the time-delay can be measured from deep and sharp images (and spectra), but we have not paid much attention, so far, on the gravitational part of the time-delay. It depends on the mass surface density distribution $\Sigma(\vec{\theta})$ of the lensing object(s), which can not be measured directly. It has therefore to be *modeled*, and getting a "realistic" estimate of $\Sigma(\vec{\theta})$ is not trivial.

A good lens model should in principle be able to reproduce the observables with as few free parameters as possible. Ideally, this model should be unique. It is "asked" to reproduce the astrometry of the quasar images with a very high accuracy, as well as their flux ratios. In fact we will not consider the latter as a strong constrain. Even if flux ratios can be measured with an accuracy of the order of the percent, they are affected by extinction by dust and by microlensing events due to the random motion of stars in the lensing galaxy (see Schechter 2003; Wambsganss 2003). Flux ratios may therefore vary with time and wavelength. In addition, they should be corrected for the effect of the time-delay, i.e., each quasar image should be measured when the quasar is seen in the same state of activity. This can be done for quasars with known time-delays and well measured light curves. Curiously, such a correction is not much taken into account in the literature, even for quasars with known time-delays.

When modeling lensed quasars, one is asked, on the basis of a few (usually 2 or 4) quasar images, to model the whole two-dimensional gravitational potential of the lensing galaxy or galaxies. There is of course no unique solution to the problem: too few observational constraints are available and several mass models giving each one a different time-delay can reproduce a given image configuration, its astrometry and flux ratios. In other words, lens models are *degenerate*.

Degeneracies have been described and blamed abundantly in the literature for being the main source of uncertainty in lens models (see for example Saha 2000; Wucknitz 2002). Whatever precision on the measured astrometry and time-delay, several mass models will predict several time-delays and hence several H_0. One must devise techniques to break the degeneracies or find quasars that are less affected by them.

The main degeneracy one has to face in quasar lensing is called the *mass sheet degeneracy*: when adding to a given mass model, a sheet of constant mass density (i.e., constant convergence κ, as defined in the preceding chapters), one does not change any of the observables, except for the time-delay. The additional mass can be internal to the lensing galaxy (e.g., ellipticity does not change the total mass within the Einstein radius, but does change κ at the position of the images) or due to intervening objects along the line of sight. The exact mass

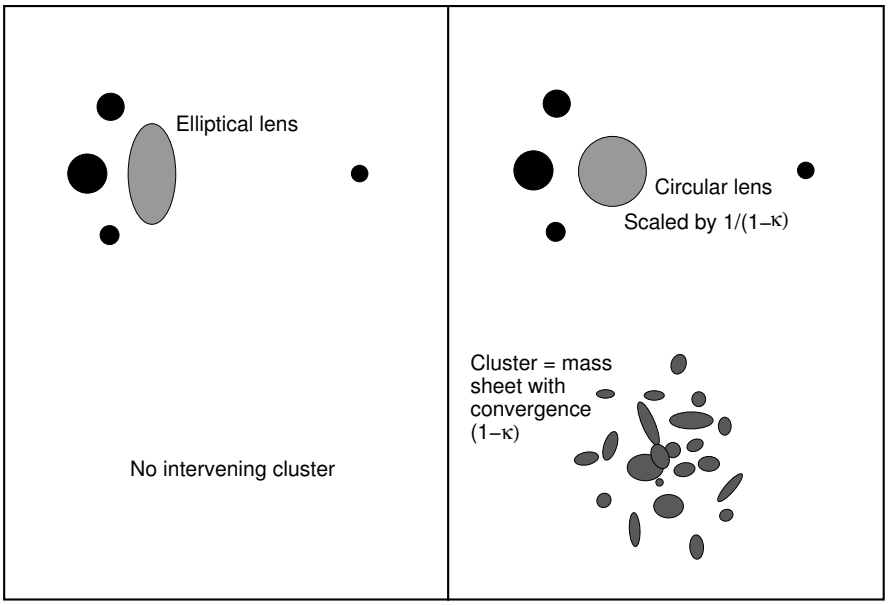

Figure 4. Two ways of obtaining a given image configuration. The left panel displays a system with four images, with an elliptical lens that introduces convergence and shear at the position of the images. On the right panel, is shown the same image geometry and flux ratios, but the lens is now circular. One would in principle only obtain two images with such a lens. The shear required to obtain four images is introduced by the nearby cluster. The mass density of the cluster is represented through its convergence κ. The mass of the main lens is scaled accordingly by $1/(1\text{-}\kappa)$ so that the image configuration remains the same as in the left panel: the mass in the main lens and in the cluster are degenerate. If no independent measurement is available for at least one of the components (main lens or cluster), it is often difficult to know, from the modeling alone, what exactly are their respective contributions.

introduced by the mass sheet increases the total mass of the lens, but one can re-scale it and locally change its slope at the position of the images. The result is that the image configuration does not change, but the convergence κ, at the position of the images does change, and modifies the time-delay. Therefore, knowledge of the the *slope* of the mass profile of the lensing galaxy, whether it be under the form of a model or of a measurement, is one of the keys to the determination of a "good" model.

Changing the slope of the lens will change κ at the position of the images, but adding intervening objects along the line of sight to the lens has a similar effect. A group or cluster of galaxies, located angularly close to the lens, will add its own contribution to the total mass density at the position of the images. If the group/cluster has a constant density κ, rescaling the total mass of the lensing

galaxy by $1/(1-\kappa)$ will leave the observed images configuration unchanged, as illustrated in Fig. 4, but will change the time-delay.

Adding convergence also modifies the shear γ, hence the ellipticity of the main lens. There are therefore several ways of reproducing a given combination of shear and convergence at the position of the images, as illustrated in Fig. 4. In the left panel of the figure, the shear γ, is produced only by the main *elliptical* lensing galaxy. In the right panel, the total shear is a combination of the lens-induced shear and of that of the nearby galaxy cluster. In principle, it is even possible to model a given system equally with either one single elliptical lens or with a completely circular lens and an intervening cluster responsible for an "external" source of shear.

Both types of degeneracies can be broken or, at least, their effect can be strongly minimized, by constraining in an independent way (1) the mass profile of the main lens, and (2) the total mass (and possibly also the radial mass profile) of any intervening cluster along the line of sight. This work can be done with detailed imaging, spectroscopy of all objects along the line of sight, and by using numerical multi-components models for the total lensing potential. This is the topic of the next section, illustrated through the example of the well studied quadruple PG 1115+080.

4. PG 1115+080: a Clean Quadruple

PG 1115+080 is one of the first case of quadruply imaged quasar (Weymann et al. 1980) and among the best studied lensed quasars, one of the still rare systems with well measured time-delays (Schechter et al. 1997). The tremendous gain in spatial resolution achieved since the eighties (see Fig. 5), has allowed detailed understanding of the system. Since the range of observational data available for PG 1115+080 is so broad, we take this object as an example to show how observations help to pin down the Hubble parameter H_0.

PG 1115+080 is a bright quasar at z=1.722, with a relatively "wide" angular separation between its images, of the order of $2''$. Two images are isolated (B and C in Fig. 5) and a blend of two brighter images, is located on the other side of the lens in projection on the plane of the sky (A1/A2 on Fig. 5). This blend A1/A2 was not resolved on the discovery images of the object, and PG 1115+080 was subsequently believed to be a triple until more detailed observations revealed it was in fact a quadruple (Young et al. 1981). Applying Refsdal's method (1964) to PG 1115+080 has been a long process. Some of the ingredients necessary to the lens modeling had to wait for years before suitable observations finally became available.

4.1. Redshifts

As already mentioned, the redshift of the lensing galaxy $z_{\rm L}$ is mandatory for the determination of any model. Although PG 1115+080 was discovered in 1980, it is only in 1997 that $z_{\rm L}$ was measured (Kundic et al. 1997), by using the Keck telescope. The galaxy is at low redshift, $z_{\rm L} = 0.311$. With deeper exposures, its velocity dispersion has also been measured, $\sigma_{\rm L} = 281 \pm 25$ km.s^{-1} as well as the velocity dispersion of a group of galaxies found along the line of sight (Fig. 6), $\sigma_{\rm grp} = 326$ km.s^{-1} (Tonry 1998). These measurements provide us with an

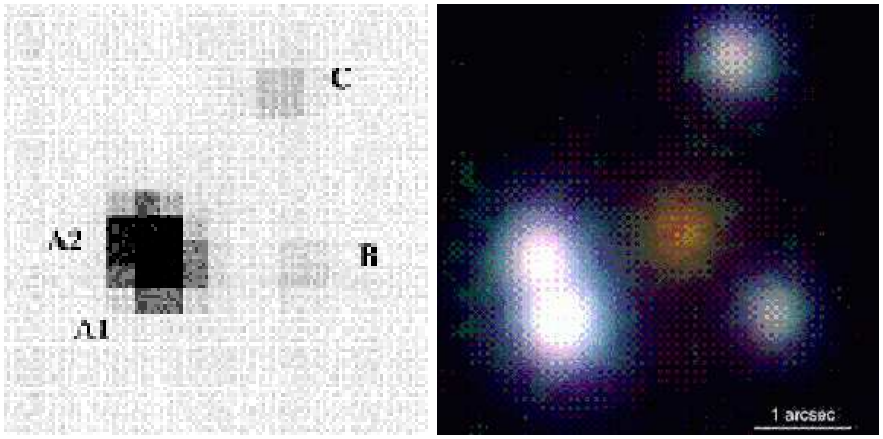

Figure 5. *Left*: ground based image of PG 1115+080 adapted from Schechter et al (1997), with a field of view of 5″ on a side. The data, with a resolution of about 0.8″, is of sufficiently good quality for measuring the photometric variations of the quasar images. It is however not good enough to obtain detailed surface photometry of the lensing galaxy. *Right:* one of the very best images ever obtained of PG 1115+080, with the 8.2m Subaru telescope. The image has a resolution of 0.32″, approaching that of the Hubble Space Telescope (Iwamuro et al. 2000), and allowing for precise measurements of the quasar and lens astrometry as well as for detailed surface photometry of the lens.

independent estimate of the total mass of the lens and intervening group. They are crucial when trying to break the mass sheet degeneracy.

4.2. Time-delays and Temporal Sampling

With its bright images, its wide angular separation, and with the availability of reference stars within a few arc-minutes, PG 1115+080 is an excellent target for photometric monitoring. Excellent does not automatically imply easy ! Photometric monitoring still requires good seeing, at least a medium size telescope (2m) and a temporal sampling adapted to the observed variations.

Choosing the temporal sampling of the light curves is critical. It is often claimed that it should be smaller than half the expected time-delay, but this is not quite true. The measurement of the time-delay is done through the measurement of the photometric variations of the quasar itself. Therefore, the sampling should be chosen according to the typical time-scale observed or expected in the photometric light curves. In an ideal case where the intrinsic variations of the source are slow compared with the time-delay, one can in principle chose a sampling even larger than the time-delay. The situation is quite the same than in image processing where one can measure the position of an object on a CCD frame with a much higher accuracy than the sampling adopted to represent this signal.

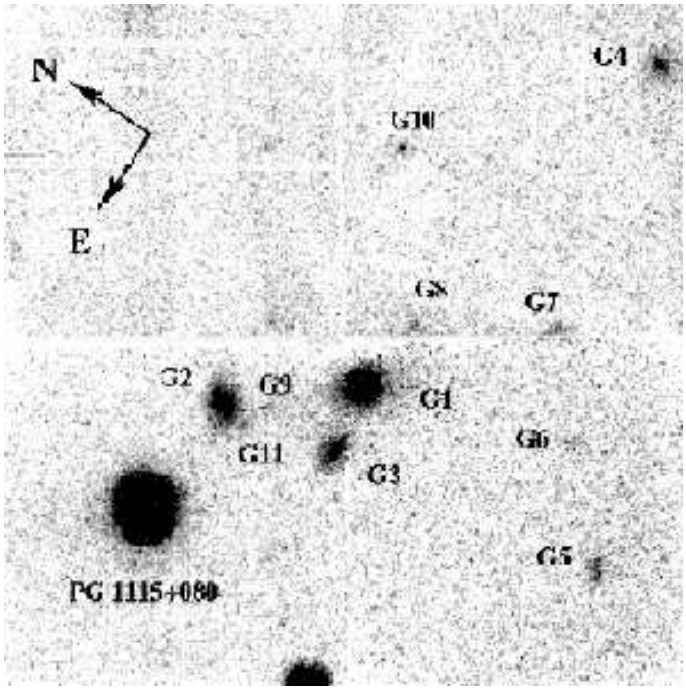

Figure 6. Infrared image of PG 1115+080, taken with the HST and the NICMOS camera (Impey et al. 1998). The field of view is 35″ on a side and shows several "companions", projected on the plane of the sky. The galaxies labeled "G" are part of a group to which also belongs the main lensing galaxy PG 1115+080. These galaxies have to be taken into account when modeling the potential well responsible for the image configuration.

However, while one do not need in principle very high temporal sampling, the situation in practice is just the opposite. First, one does not know in advance what the time-scale of the variations will be: the frequency range in quasar variability spans from days to weeks or even months. Second, even if the variations are slow, their amplitude is small, often of the order of a few tens of a magnitude, sometimes a bit more in the case of Broad Absorption Lines (BAL) quasars. Measuring faint variations is easier with well sampled light curves. Well sampled curved are, in addition, well suited to the use of cross-correlation techniques in order to measure the time-delay. Finally, microlensing by stars in the lensing galaxy introduces flickering of the light curves, with a frequency that is in general unknown and not even easy to predict before the data are actually taken. There is therefore no general line to adopt on the choice of the sampling other than trying to get "the finest possible sampling" !

The case of PG 1115+080 is lucky enough that the photometric variations of the source are slow, and well sampled light curves could be obtained (Schechter et al. 1997; see Fig. 7). Even with light curve of such a quality, extracting the

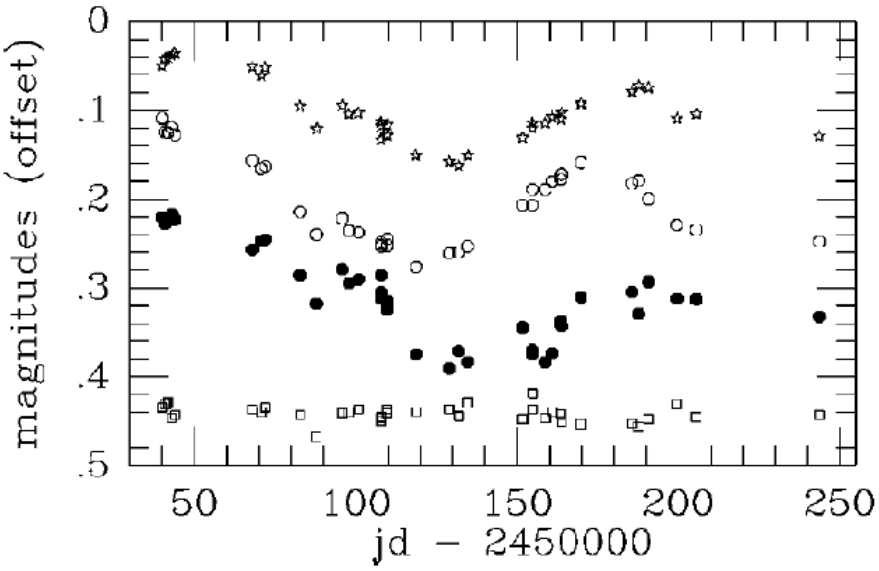

Figure 7. Optical V-band light curves for the different components of PG 1115+080. From top to bottom, the curves for the blend A1/A2, component C, component B, and a reference star (Schechter et al. 1997). Note the smooth and slow variation of the quasar, the absence of high frequency flickering, as would introduce microlensing, and the striking similarity between the light curves.

time-delay(s) can be tricky. Schechter et al. (1997) uses the method devised by Press et al. (1982) to compute a global χ^2 between shifted versions of the light curves. They estimate the time-delay between components C and B to be $\Delta t(CB) = 23.7 \pm 3.4$ days and the time-delay between component C and A is $\Delta t(CA) = 9.4$ days, where C is always the first one to vary, i.e., the "leading image". A different approach was chosen by Barkana (1997) to analyse the same data. Using an analytical representation of the light curves and taking into account the correlations between the errors on the individual photometric measurements, they derive a very similar time-delay between components C and B, $\Delta t(CB) = 25^{+3.3}_{-3.8}$ but the second time-delay is significantly longer $\Delta t(CA) =$ 13 days.

4.3. Modeling and Influence of the Astrometry

Using a simple isothermal model plus external shear (induced by the cluster) Schechter et al. (1997) infered $H_0 = 42$ km.s^{-1}.Mpc^{-1}, but no detailed observations of the lensing galaxy was available at that time. In fact, Schechter et al. (1997) found that a value as high as 84 was possible as well. Keeton & Kochanek (1997) investigated analytical models for the lensing galaxy, including isothermal profiles and softened power laws with core radius. They found that the potential well in PG 1115+080 could not be modeled using a single lensing

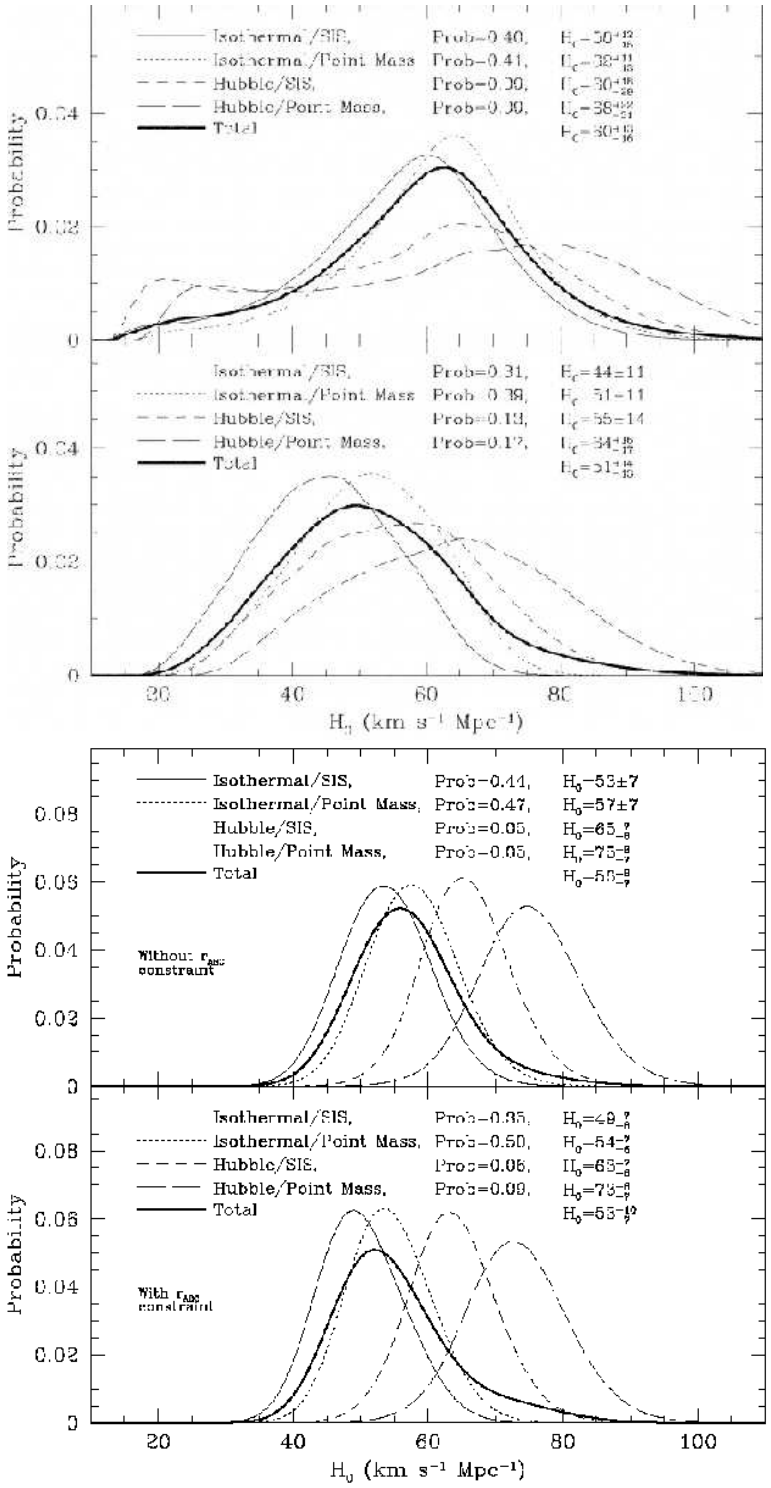

Figure 8. *Top:* probability density for H_0 using the models of Keeton & kochanek (1997), for various combinations of models for the main lens and intervening group and using one time-delay (top panel) or two time-delays (bottom panel). *Bottom:* Same as above but using improved astrometry (Courbin et al. 1997).

galaxy, whatever its mass profile. External shear by the nearby group had to be invoked. A combination of models were tested for the main lens and for the cluster, and analyzed in a statistical way in order to derive a probability density for H_0. The experiment is done in two ways: by taking into account only one time-delay in PG 1115+080, and by using the two measured time-delays.

The models by Keeton & Kochanek are based on astrometry obtained with HST data, before the optics was refurbished (Kristian et al. 1993), and with rather large astrometric errors. As systems with symmetric image configurations about the lens are more sensitive to errors on the astrometry than assymetric ones, the result by Keeton & Kochanek could be improved further, simply by improving the HST astrometry. This was done by applying deconvolution techniques to ground based images of PG 1115+080. Fig. 8 illustrates the gain in the accuracy. With the new astrometry, not only the width of the probability distributions is decreased, but there is also better agreement between the curves obtained for one and for two time-delays. The combined probability for the pre-refurbishment HST astrometry is H_0 of 51^{+14}_{-10} km.s^{-1}.Mpc^{-1}while $H_0 = 53^{+10}_{-7}$ km.s^{-1}.Mpc^{-1}with the improved astrometry.

In parallel with the efforts to improve the observational constraints for PG 1115+080, new models were developed, with the aim of exploring more of the parameter space defined by the slope of the mass profile of the lens, its ellipticity and its position angle. One approach to the problem is to consider a family of non-parametric models, where the lensing galaxy is decomposed on a grid of mass "pixels" or tiles. The astrometry, flux ratios, and time-delays are given as observational constraints, and the output of the procedure is a pixelized mass map of the lens, as well as its slope. As is done for parametric models, one can have a statistical approach and run many models in order to infer a probability density for H_0 (Williams & Saha 2000). As the range of possible models is much broader with the non-parametric approach than with the parametric one, it was found that H_0 could be anything between 42 and 84, given the observations available for PG 1115+080 at that time (Saha & Williams 1997) !

4.4. HST Imaging: the Quasar Host Galaxy

Improving the astrometry over and over, helps, but does not solve the fundamental problem imposed by the mass sheet degeneracy. The number of lensed images available can not be increased, so that potential well of the lens, and hence the arrival-time surface, are probed only at a very limited number of points. This is quite not true as soon as one considers extended sources. Quasars have host galaxies. They are faint, but they have a much larger angular size than the quasar they harbourgh. The effect of lensing on their shape, distorted and stretched, is much stronger than on the point source quasar. The role of high angular resolution observations therefore extends well beyond the simple aim of measuring the image positions and fluxes. Each detail discovered in the lensed image of the host galaxy is an additional point in the mass map.

PG 1115+080 has been observed with the refurbished HST, in the infrared (Impey et al. 1998), with a resolution and depth sufficient to unveil an almost full ring joining the quasar images (Fig. 9). While the host galaxy provides more constraints for the models, it also forces to introduces more degrees of freedom.

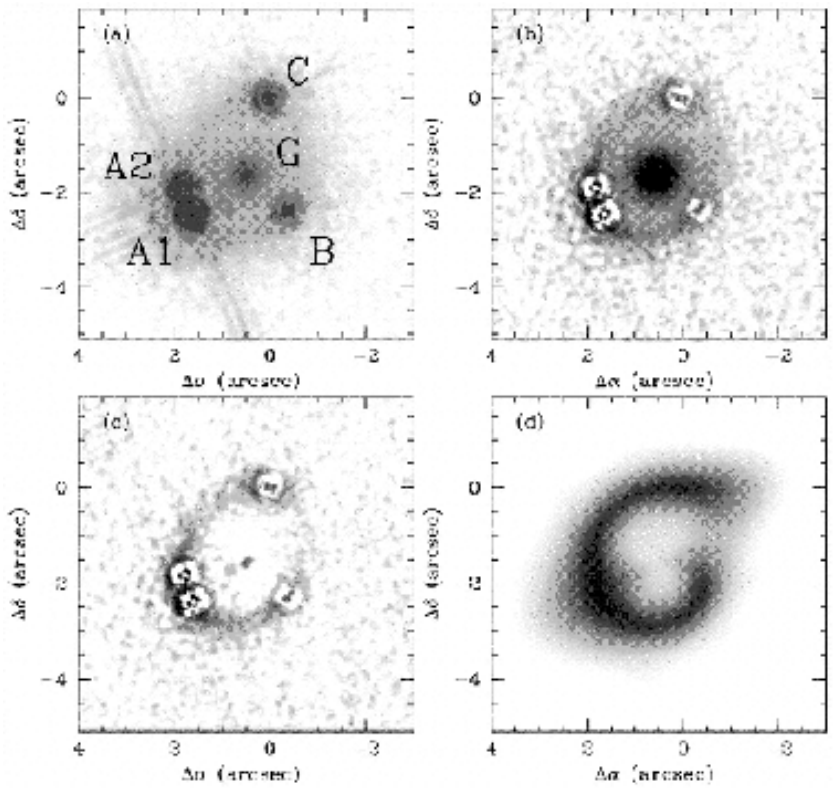

Figure 9. An HST image of PG 1115+080 is shown in the upper left panel (Impey et al. 1998), with the four quasar images and the lens G. Removal of the quasar images, as done in the upper right panel, unveils an almost full ring: the lensed host galaxy of the quasar. It is even more evident after removal of the lensing galaxy, in the lower left panel. If a model is adopted for the "unlensed" host galaxy, the shape of the lensed ring can be predicted (lower right panel), and compared with the observations.

Indeed, a model has to be *chosen* to represent the "unlensed" host, for example an exponential disk, as done in Impey et al. (1998). Feeding the lensing model with the image positions, time-delays, flux ratios, lens ellipticity, position of the nearby group of galaxies, and the model for the host, one can reproduce the observed ring.

The actual gain brought by the ring is significant but not always sufficient to discriminate between lens models. Impey et al. (1998) give two estimates for H_0 for two different type of lens models. One assumes that light traces mass, i.e., that the mass-to-light ratio is constant in every point of the lens. The second, more realistic according to our current knowledge of the mass distribution in galaxies, includes a dark halo component. Using these two models, they find H_0 = 66 km.s^{-1}.Mpc^{-1}and H_0 = 44 km.s^{-1}.Mpc^{-1}, respectively.

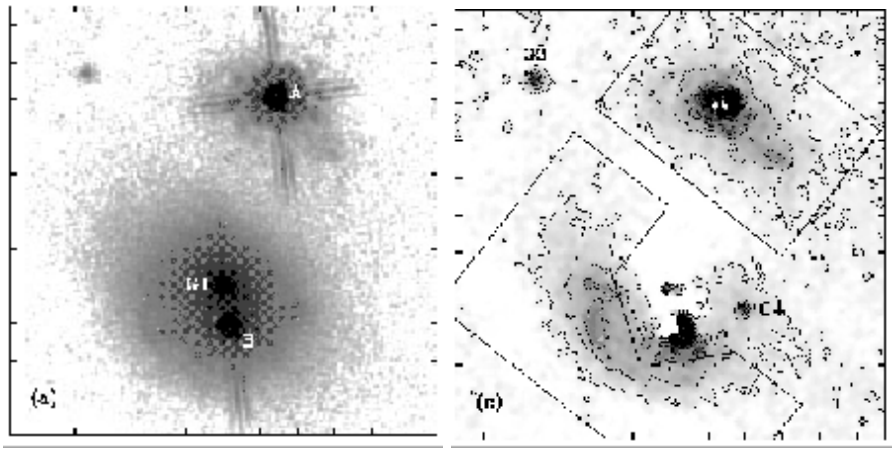

Figure 10. *Left:* HST NICMOS observation obtained by the CASTLE group, where the two quasars and the lensing galaxy are well separated. *Right:* the quasars and the lens have been removed to unveil the host galaxy of Q 0957+561. On the contrary of PG 1115+080, many details are seen in each image of the host (Keeton et al. 2000).

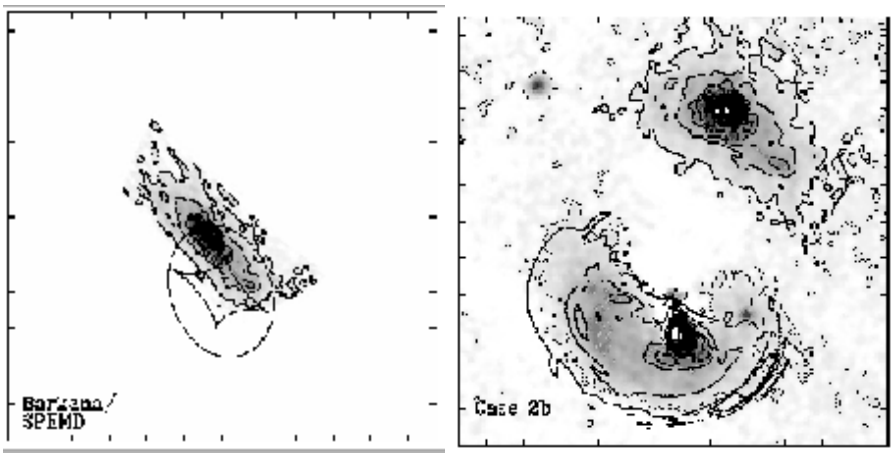

Figure 11. *Left:* the A image of the host is mapped back into the source plane to reconstruct the unlensed image of the host. *Right:* the source is imaged again in order to produce image B given the lens model. The image B, as predicted by the model, is the solid contour in the figure. Grey levels are the observations (Keeton et al. 2000).

A complete Einstein ring was found in PG 1115+080, but with no resolved details, only the surface brightness can be used to constrain the models. Because the of the high degree of symmetry of the system, and given the resolution of the observations, it is not clear whether full rings are actually useful for sorting out between different mass models, or not (see, e.g., Saha & Williams, 2001).

Many other lensed hosts galaxies have been discovered using HST images (Lehar et al. 2000), in systems that are less symmetric than PG 1115+080, and with higher degree of detail. A good example is the double Q 0957+561 in which the host galaxy reveals clumps, distorted arcs and for which a different approach of the modeling was used, not involving any prior model for the host's surface brightness (Keeton et al. 2000). Since the observations of the host of Q 0957+561 are probably the most detailed existing so far, we will briefly leave PG 1115+080 aside and use Q 0957+561 to illustrate the use of hosts in quasar lensing. The observations are shown in Fig. 10, while Fig. 11 illustrates the modeling method. Based on the image of the brighter component A of the host, mapping it back onto the source plane, the unlensed host is reconstructed. It is then re-imaged, in order to produce the fainter image B, and a χ^2 is minimized, between the observed image and the prediction from the model. The method takes advantage of the high degree of details in the host, and on the assymetric configuration of the system. It does not require any strong prior knowledge on the host. The method allows to rule out several models previously published in the literature.

4.5. Yet Further Constraints: Spectroscopy

So far, and mainly for technical reasons, the most important constraints on lens models were coming from imaging. Spectroscopy is nevertheless another key component, that will become of growing importance in the near future, thanks to 3D spectrographs mounted on large telescopes.

Spectroscopy provides independent access to the total mass of the lenses: whenever an intervening cluster or group is seen close to the line of sight to a lens, measuring its velocity dispersion helps to break the mass sheet degeneracy it introduces with the mass of the main lens (e.g., Falco et al. 1997; Tonry 1998; Kneib et al. 2000). If a measurement of the velocity dispersion of the main lens is available as well, the effect of the mass sheet degeneracy is greatly minimized In the case of PG 1115+080, both the velocity dispersion of the main lens and nearby group are available (see Table 1).

For an isothermal sphere the line of sight velocity dispersion σ is directly related to the Einstein radius, through the H_0 independent relation:

$$\theta_{\rm E} = 4\pi \frac{\sigma^2}{c^2} \frac{D_{\rm L}}{D_{\rm S}} \tag{6}$$

Since the Einstein radius $\theta_{\rm E}$ only depends on the total mass of the lens (within the Einstein radius), measuring the velocity dispersion does not yield the mass profile of the lens. Nevertheless, it can be used to put strong constraints on the mass profile, using further knowledge we have on galaxies in general. Treu & Koopmans (2002) take the problem under this view angle and feed dynamical models of galaxies with the measured velocity dispersions in PG 1115+080. In their model, the lensing galaxy is composed of a dark matter halo with a mass density profile of the form $\rho(r) = r^{-\gamma}$ ($\gamma = 1$ for a Navarro, Frenk & White (1997) profile) and a Jaffe stellar density profile (Jaffe 1983). New parameters appear in the model: the slope γ or the dark matter halo, and the fraction of the galaxy that is under the form of (luminous) stars, $f_\star$. However, (γ, $f_\star$) define a parameter space with a rather sharp peak, centered at $\gamma \sim 2.35$ and $f_\star \sim 0.67$,

for PG 1115+080. There is therefore a rather small range of lens models that fit simultaneously the physical properties of the lens, and the constraints imposed by lensing. Using this approach leads to $H_0 = 59^{+12}_{-7}$ km.s^{-1}.Mpc^{-1}, a value which is much less affected by systematic errors than other estimates, not taking the dynamical information into account.

Measuring velocity dispersions in faint objects in not easy, especially when they are blended with bright quasar images. It has been possible, so far, only for a few systems, but spectrographs are starting to be used on large telescopes where adaptive optics observations are carried out in a flexible way. Three-dimensional spectrographs are planed on these telescopes, and may well yield not only the velocity dispersion of lenses, but also their full velocity field. In many cases, one will be able to measure at least the velocity dispersion profile, hence constraining much better the mass profile of the lens, independent of lensing.

4.6. H_0 with PG 1115+080

Although many lensed quasars are potentially as powerful as PG 1115+080 for constraining H_0, this nice quadruple remains one of the best studied cases so far, along with the double Q 0957+561. Basically all possible observational tools have been used to study PG 1115+080, and we have adopted it as an example to illustrate how observations help the theorist in quasar lensing. Some of the main results obtained for PG 1115+080 are summarized in Table 1, following the chronological order of the observational saga of the object.

As the observations of PG 1115+080 were improving, various values were found for H_0 along the years. This is mainly a consequence of the mass sheet degeneracy and to the lack of observational constraints on the actual mass profile of the lens. Among the range of possible values, the highest ones were obtained for lenses with constant mass-to-light ratios, and lower values of H_0 were found for models including a dark matter halo. If our knowledge of the physics of galaxies is any good, the latter lens model is closer to the truth than the former. This results in values for H_0 that disagree (see Table 1) with local estimates, based on standard candles, i.e., $H_0 = 72 \pm 8$ km.s^{-1}.Mpc^{-1} (Freedman et al. 2001).

5. Mass Production of Time-Delays: H_0 with Other Lenses

Measuring time-delays has long been the main limitation to the use of quasar lenses in cosmology. Indeed, obtaining on a regular basis images of good quality and for long period of time is not easy. With the increasing number of large telescopes in excellent sites, and operated in "service mode", we have nevertheless entered a phase of mass production of time-delays. It took more than a decade to obtain the time-delay in Q 0957+561, but four time-delays were recently measured in one single thesis (Burud, 2000b) thanks to modern instrumentation and image deconvolution techniques. In addition, systematic imaging campaigns of lensed quasars such as the one carried out by CASTLE, facilitate the modeling of lens galaxies. Deep HST images are used in combination with spectroscopy, and along with what we know of the physics/dynamics of galaxies, to break the degeneracies between the models.

Table 1. Summary of the observational saga of PG 1115+080 since the time-delay measurement, and estimates for H_0 (along with the 1σ errors, when available) while the observations improve.

Reference	Observational or theoretical improvement	H_0 ($km.s^{-1}.Mpc^{-1}$)
Schechter et al. (1997)	Time delay measurement: $\Delta(CB) = 23.7 \pm 3.4$ days $\Delta(CA) = 9.4$ days	42 or 84
Barkana (1997)	Redetermination of time-delays (Schechter's data): $\Delta(CB) = 25^{+3.3}_{-3.8}$ days $\Delta(CA) = 13$ days	no new estimate
Kundic et al. (1997)	Redshifts of the lens and group: $z_{lens} = z_{group} = 0.311$ $\sigma_{group} = 270 \pm 70$ km/s	52±14
Saha & Williams (1997)	Non parametric models including main lens plus group. Explore broad range of lens mass profiles and ellipticities.	42, 63, or 84
Keeton & Kochanek (1997)	Parametric models including main lens and group. Explore broad range of lens shapes.	51^{+14}_{-13}
Courbin et al. (1997)	Improved astrometry from ground based imaging.	53^{+10}_{-7}
Impey et al. (1998)	New HST/NICMOS images. Discover lensed ring. Improved astrometry and lens ellipticity.	44 ± 4 or 65 ± 5
Tonry (1998)	Velocity dispersion of the lens and group: $\sigma_{lens} = 281 \pm 25$ km/s $\sigma_{group} = 326$ km/s	
Treu & Koopmans (2002)	Use dynamical info on the lens and group to break degeneracies between models	59^{+12}_{-7} (± 3 syst)

Table 2. Summary of measured time-delays, given with respect to the leading image. When several measurements have been obtained, we only give the more recent one. The 1σ error as well as the relative error on the time-delay are given. The third column displays the value infered for H_0 for each system and the 1σ error. In most cases we have considered the value given in the paper where the time-delay was published. When H_0 has been obtained by other authors, the reference is given as well.

Object	Time-delay(s) (leading image first)	H_0 ($km.s^{-1}.Mpc^{-1}$)
B 0218+357		
Biggs et al. (1999)	$\Delta(BA) = 10.5\pm0.2$ days (2%)	69^{+7}_{-9}
RX J0911+0551		
Hjorth et al. (2002)	$\Delta(BA) = 146\pm4$ days (3%)	71 ± 2 (±4 syst)
Q 0957+561		
Kundic et al. (1997)	$\Delta(BA) = 417\pm0.6$ days (0.15%)	64 ± 7
	but multiple time-delays	
Goicoechea (2002)	$\Delta(BA) = 425\pm4.0$ days (1.0%)	
	$\Delta(BA) = 432\pm1.9$ days (0.5%)	
HE 1104−1805	Strong micro/milli-lensing	
Gil-Merino et al. (2002)	$\Delta(AB) = 310\pm9$ days (3%)	48 ± 2 or 62 ± 2
PG 1115+080		
Schechter et al. (1997)	$\Delta(CB) = 25^{+3.3}_{-3.8}$ days (14%)	
Barkana (1997)	$\Delta(CA) = 13$ days	
Treu & Koopmans (2002)		59^{+12}_{-7} (±3 syst)
SBS 1520+53		
Burud et al. (2002)	$\Delta(BA) = 130\pm3$ days (3%)	51 ± 9
B 1600+434	Radio and optical time-delays	
Koopmans et al. (2000)	$\Delta(BA) = 47\pm5$ days (10%)	57^{+7}_{-6}
Burud et al. (2000)	$\Delta(BA) = 51\pm2$ days (4%)	52^{+7}_{-4}
B 1608+656		
Fassnacht et al. (2002)	$\Delta(BA) = 31.5\pm2$ days (6%)	63 ± 15
	$\Delta(BC) = 36.0\pm2$ days (6%)	
	$\Delta(BD) = 77.0\pm3$ days (4%)	
PKS 1830−211		No estimate. Lens
Lovell et al. (1998)	$\Delta(BA) = 26^{+4}_{-5}$ days (17%)	may be multiple
HE 2149−2745		
Burud et al. (2002b)	$\Delta(BA) = 103\pm12$ days (11%)	65 ± 8
COMBINED		**61±7**

Even if the observational situation in quasar lensing is expected to improve a lot in the coming years, thanks to adaptive optics and 3D spectrographs, we can already say, with the precision of the observations collected so far, that lensed quasars are at least as powerful as other methods to determine H_0.

Let us play the naive game that consists in taking from literature the nine estimates of H_0, for each of the nine measured time-delays, and average them. This is summarized in Table 2 for all known lenses, along with the time-delay measurements. We indicate in the table the value obtained for H_0 with all kind of different models, just scaling the published errors to 1σ. Some authors consider isothermal spheres or ellipsoids with and without external shear. Others prefer to use lenses with constant mass-to-light ratios. In other words, the values we quote in Table 2 are all affected by unknown systematics. These systematics have been estimated by each author and included in the published error bars. If they had been under- or over- estimated, the dispersion between all the individual estimates of H_0, and the published errors on one single measurement, would be incompatible. Following our naive idea the averaged value for H_0, (without error weighting) is H_0=61$\pm$7 km.s^{-1}.Mpc^{-1}. Figure 12 is another way of displaying the data of Table 2, showing the value of H_0 as a function of the lens redshift. The 1σ error region is dashed on the figure. Four measurements (in fact 3, if we include the mean value for the 2 estimates for HE 1104-1805 in the dashed area) are outside the 1σ region, as expected for 9 independent measurements. Unless all the authors did the same systematic error (and this is unlikely because of the very different choices of models), the dispersion between the points is fully compatible with the individual error bars. This means that even if the models suffer from systematics, the amplitude of the error has been correctly estimated by the authors.

A more correct approach is to impose that a given family of profiles is used to model the mass distribution of lenses in general, and to impose that H_0 should be the same everywhere in the Universe. This has been done so far by very few authors. Williams & Saha (2000), use two systems and their non-parametric models, to infer H_0=61$\pm$11 km.s^{-1}.Mpc^{-1}(1σ error). Courbin et al. (2002) add two other lenses to the Williams & Saha sample, and adopt the same non-parametric technique to infer H_0=64$\pm$4 km.s^{-1}.Mpc^{-1}. Using parametric lens models and a set of 4 *different* lenses (only PG 1115+080 is common to all authors) Kochanek (2002) obtain H_0=51$\pm$5 km.s^{-1}.Mpc^{-1}if lens galaxies have dark matter halos, or H_0=73$\pm$8 km.s^{-1}.Mpc^{-1}if lens galaxies have constant mass-to-light ratios.

Gravitationally lensed quasars have one drawback over other methods for determining H_0: they do require good knowledge of the mass profile of the lens. It has long been a limitation to the effectiveness of the method to produce reliable estimates of H_0, but this drawback is becoming easier and easier to overcome, thanks to spectroscopy, to high spatial resolution observations, and to the progresses made on the physics of galaxies. Gravitational lenses have, on the other hand, tremendous advantages over other methods. First, they do not rely on any "standard candle" which would rend the method close to useless if the standard candle turned out to be significantly deviant from the "standard" behaviour. Second, it does not require secondary calibrators of the standard candle, e.g., low redshift objects, in the case of the supernovae method. Third,

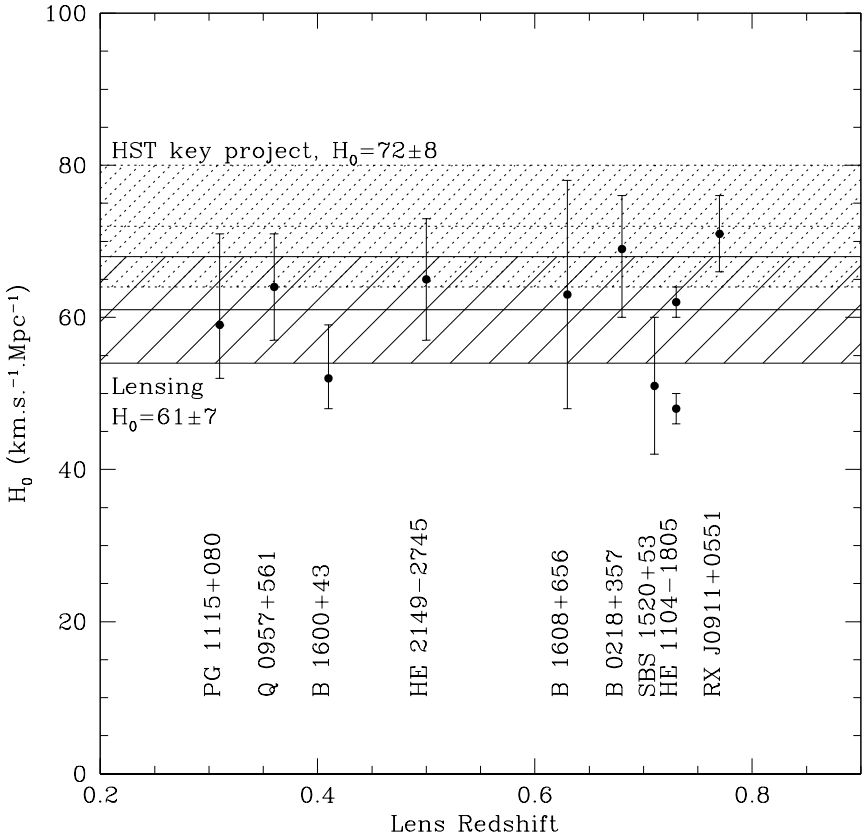

Figure 12. Values of H_0 for all lenses with known time-delays. H_0 is given as a function of lens redshift, directly taken from the literature. The dashed area shows the range of possible values, according to lensing, which is to be compared with the dashed-dotted area, infered from the Cepheid method in the framework of the HST key project. As in the case of PG 1115+080, the mean value for H_0 is very marginally compatible with the local estimate of the Hubble parameter.

it probes H_0 at cosmological distances, independent of any local effect such as peculiar velocities of nearby galaxies. Finally, lensing is not as sensitive to the other cosmological parameters (Ω_m, Ω_Λ) than the other methods.

We compare in Fig. 12, the value of H_0 for lensed quasars and for the Cepheid method. With the present error bars, calculated with only 9 objects, we can say that lensed quasars and Cepheid disagree. Lensing gives lower values for H_0 than does the Cepheid method. If our knowledge of the mass distribution of galaxies is any good, i.e., that galaxies have dark matter halos, the lensing value would be even smaller. Recent CMB experiments such as WMAP find high

values for H_0 (e.g., Spergel 2003), in agreement with the local estimate: H_0=71, with impressive error bars of only 4%. With the high degree of degeneracy between the cosmological models used to represent the observed CMB power spectrum, H_0 is in fact shown to take any value between 54 and 72 (Efstathiou 2003). It spans over an even broader ranger if one does not invoke any prior knowledge on the value of Ω_m and Ω_Λ as determined with supernovae.

In fact, no single method has been proved to be good enough that it can surpass the others. There are, however, methods that are better than others as pinning down *some* of the cosmological parameters and it has been emphasized many times (Bridle et al. 2003) that all methods should be combined in order to break the degeneracies inherent to one specific method. Gravitational lensing is one of these methods. It has advantages and drawbacks, but probably many more advantages than drawbacks given the present observational context.

Acknowledgments. The author wishes to thank Alain Smette and Pierre Magain for useful discussions. Frédéric Courbin is supported by the European Commission through a Marie Curie Individual Fellowship, under grant MCFI-2001-0242. The collaborative grant ECOS/CONICYT C00U05 between Chile and France is also gratefully acknowledged.

References

Barkana, R. 1997, *ApJ*, **489**, 21

Biggs, A.D., Browne, I.W.A., Helbig, P., et al. 1999, *MNRAS*, **304**, 349

Bridle, S.L., Lahav, O., Ostriker, J.P., et al. 2003, astro-ph/0303180

Burud, I., Hjorth, J., Jausen, A.O., et al. 2000, *ApJ*, **544**, 117

Burud, I., 2000, PhD, Liège University, Belgium

Burud, I., Hjorth, J., Courbin, F., et al. 2002, *A&A*, **391**, 481

Burud, I., Courbin, F., Magain, P., et al. 2002b, *A&A*, **383**, 71

Courbin, F., Magain, P., Keeton, C.S., et al. 1997, *A&A*, **324**, L1

Courbin, F., Saha, P., Schechter, P.L. 2002, in *"Gravitational Lensing: An Astrophysical Tool"*, LNP topical volume 608, (eds. Courbin, Minniti), p1

Efstathiou, G. 2003, astro-ph/0303127

Falco, E.E., Shapiro, I.I., Moustakas, L.A., et al. 1997, *ApJ*, **484**, 70

Fassnacht, C.D., Xanthopoulos, E., Koopmans, L.V.E., et al. 2002, *ApJ*, **581**, 23

Freedman, W.L., Madore, B.F., Gibson, B.K., et al. 2001, *ApJ*, **553**, 47

Gil-Merino, R., Wisotzki, L., Wambsganss, J. 2002, *A&A*, **381**, 428

Goicoechea, L. J. 2002, *MNRAS*, **334**, 905

Hewitt, J.N., Turner, E.L., Lawrence, C. R., et al. 1992, *AJ*, **104**, 968

Hjorth, J., Burud, I., Jaunsen, A.O., et al. 2002, *ApJ*, **572**, L11

Huchra, J., Gorenstein, M., Kent, S., et al. 1985, *AJ*, **90**, 691

Impey, C.D., Falco, E.E., Kochanek, C.S., et al. 1998, *ApJ*, **509**, 551

Iwamuro, F., Motohara, K., Maihara, T., et al. 2000, *PASJ*, **52**, 25

Jackson, N., Nair, S., Browne, I.W.A., et al. 1998, *MNRAS*, **296**, 483

Jaffe, W. 1983, *MNRAS*, **202**, 995
Keeton, C.R., Falco, E.E., Impey, C.D., et al. 2000, *ApJ*, **542**, 74
Keeton, C.R., Kochanek, C.S. 1997, *ApJ*, **487**, 42
Kneib, J.-P., Cohen, J.G., Hjorth, J. 2000, *ApJ*, **544**, L35
Kochanek, C.S. 2002, *ApJ*, **578**, 25
Kochanek, C.S., Falco, E.E., Impey, C., et al. 2003a, the CASTLE database, `http://cfa-www.harvard.edu/glensdata/`
Kochanek, C.S. 2003b, *ApJ*, **583**, 49
Koopmans, L.V.E., de Bruyn, A.G., Xanthopoulos, E., et al. 2000, *A&A*, **356**, 391
Kristian, J., Groth, E.J., Shaya, E.J., et al. 1993, *AJ*, **106**, 1330
Kuijken, K. 2003, this volume
Kundic, T., Cohen, J.G., Blandford, R.D., et al. 1997, *AJ*, **114**, 507
Kundic, T., Turner, E.L., Colley, W.N., et al. 1997, *ApJ*, **482**, 75
Langston, G.I., Schneider, D.P., Conner, S., et al. 1989, *AJ*, **97**, 1283
Lawrence, C. R., Bennett, C. L., Hewitt, J. N., et al. 1986 *ApJS*, **61**, 105
Lehr, J., Falco, E.E., Kochanek, C.S., et al. 2000, *ApJ*, **536**, 584
Lidman, C., Courbin, F., Kneib, J.-P., et al. 2000, *A&A*, **364**, L62
Lovell, J.E.J., Jauncey, D.L., Reynolds, J.E., et al. 1998, *ApJ*, **508**, L51
Magain, P., Surdej, J., Swings, J.-P., et al. 1988, *Nature*, **334**, 327
Myers, S.T., Fassnacht, C.D., Djorgovski, S.G., et al. 1995, *ApJ*, **447**, L5
Navarro, J., Frenk, C.S., White, S.D.M. 1997, *ApJ*, **490**, 493
Patnaik, A. R., Browne, I. W. A., Walsh, D., et al. 1992, *MNRAS*, **259**, 1
Press, W.H., Rybicki, G.B., Hewitt, J.N. 1992, *ApJ*, **385**, 404
Refsdal, S. 1964, *MNRAS*, **128**, 307
Rusin, D., Marlow, D.R., Norbury, M., et al. 2001, *AJ*, **122**, 591
Saha, P., Williams, L.L.R. 2001, *AJ*, **122**, 585
Saha, P. 2000, *AJ*, **120**, 1654
Saha, P., Williams, L.L.R. 1997, *MNRAS*, **292**, 148
Schmidt, M. 1963 *Nature*, **197**, 1040
Schechter, P.L., Bailyn, C.D., Barr, R., et al. 1997, *ApJ*, **475**, 85
Schechter, P.L. 2003, this volmune
Schneider, P., Ehlers, J., Falco, E.E. 1992, in Gravitational lenses, Astronomy and Astrophysics Library, Springer-Verlag.
Schneider, D. P., Turner, E. L., Gunn, J. E. 1988, *AJ*, **95**, 1619
Spergel, D.N., Verde, L., Peiris, H.V., et al. 2003, astro-ph/0302209
Sluse, D., et al. 2003, submitted to A&A
Smette, A. 2003, this volume
Surdej, J., Magain, P., Swings, J.-P., et al. 1987, *Nature*, **329**, 695
Tonry, J.L. 1998, *AJ*, **115**, 1
Treu, T., Koopmans, L.V.E. 2002, *MNRAS*, **337**, L6

Turner, E. L. 1980, *ApJ*, **242**, L135
Vanderriest, C., Schneider, J., Herpe, G., et al. 1989, *A&A*, **215**, 1
Walsh, D., Carswell, R. F., Weymann, R. J. 1979, *Nature*, **279**, 381
Wambsganss, J. 2003, this volume
Weymann, R. J., Chaffee, F. H., Carleton, N. P., et al. 1979, *ApJ*, **233**, L43
Weymann, R. J., Latham, D., Roger, J., et al. 1980, *Nature*, **285**, 641
Williams, L.L.R., Saha, P. 2000, *AJ*, **119**, 439
Wisotzki, L., Koehler, T., Kayser, R., et al. 1993, *A&A*, **278**, L15
Wucknitz, O. 2002, *MNRAS*, **332**, 951
Wyithe, J.S., Winn, J.N., Rusin, D. 2003, *MNRAS*, **583**, 58
Young, P., Deverill, R.S., Gunn, J.E. 1981 *ApJ*, **244**, 723